Experimentally Induced Visual Projections into Auditory Thalamus and Cortex
Author(s): Mriganka Sur, Preston E. Garraghty, Anna W. Roe
Source: *Science*, New Series, Vol. 242, No. 4884 (Dec. 9, 1988), pp. 1437-1441
Published by: American Association for the Advancement of Science
Stable URL: http://www.jstor.org/stable/1702334
Accessed: 29/12/2008 11:11

Your use of the JSTOR archive indicates your acceptance of JSTOR's Terms and Conditions of Use, available at http://www.jstor.org/page/info/about/policies/terms.jsp. JSTOR's Terms and Conditions of Use provides, in part, that unless you have obtained prior permission, you may not download an entire issue of a journal or multiple copies of articles, and you may use content in the JSTOR archive only for your personal, non-commercial use.

Please contact the publisher regarding any further use of this work. Publisher contact information may be obtained at http://www.jstor.org/action/showPublisher?publisherCode=aaas.

Each copy of any part of a JSTOR transmission must contain the same copyright notice that appears on the screen or printed page of such transmission.

JSTOR is a not-for-profit organization founded in 1995 to build trusted digital archives for scholarship. We work with the scholarly community to preserve their work and the materials they rely upon, and to build a common research platform that promotes the discovery and use of these resources. For more information about JSTOR, please contact support@jstor.org.

American Association for the Advancement of Science is collaborating with JSTOR to digitize, preserve and extend access to *Science*.

http://www.jstor.org

(Digital Equipment Corporation), with custom-made analysis software. Typically, the sampling rate was 10 kHz and signals were filtered at 1.5 kHz (48 dB/octave, Bessel characteristic). Single channel openings were detected and idealized by an algorithm that used both amplitude and slope information. The amplitude of the openings and the duration of both openings and closures were stored for subsequent statistical analysis.
22. O. P. Hamill, A. Marty, E. Neher, B. Sakmann, F. Sigworth, *Pflügers Arch.* **391**, 85 (1981); D. Colquhuon and F. J. Sigworth, in *Single-Channel Recording*, E. Neher and B. Sakmann, Eds. (Plenum, New York, 1983), pp. 191–263.
23. U. Laemmli, *Nature* **227**, 680 (1970).
24. B. W. Silverman, *Density Estimation* (Chapman & Hall, New York, 1986).
25. Supported in part by NIH grants HL-31154 and DK-19318 to L.B., and NIH grants HL-37044 and HL-36930 to A.M.B. We thank G. Schuster for help with dissection and culturing of hippocampal pyramidal cells. We thank J. Breedlove, G. May, and D. Witham for their secretarial assistance.

12 July 1988; accepted 4 October 1988

Experimentally Induced Visual Projections into Auditory Thalamus and Cortex

MRIGANKA SUR,* PRESTON E. GARRAGHTY, ANNA W. ROE

Retinal cells have been induced to project into the medial geniculate nucleus, the principal auditory thalamic nucleus, in newborn ferrets by reduction of targets of retinal axons in one hemisphere and creation of alternative terminal space for these fibers in the auditory thalamus. Many cells in the medial geniculate nucleus are then visually driven, have large receptive fields, and receive input from retinal ganglion cells with small somata and slow conduction velocities. Visual cells with long conduction latencies and large contralateral receptive fields can also be recorded in primary auditory cortex. Some visual cells in auditory cortex are direction selective or have oriented receptive fields that resemble those of complex cells in primary visual cortex. Thus, functional visual projections can be routed into nonvisual structures in higher mammals, suggesting that the modality of a sensory thalamic nucleus or cortical area may be specified by its inputs during development.

WHAT IS INTRINSICALLY "VISUAL" about visual thalamus and cortex? Can visual projections be induced into nonvisual targets, and are these projections functional? The organization of the visual pathway in ferrets is similar to that in cats (*1*); the visual system of cats has been studied extensively both anatomically and physiologically. However, unlike cats, retinofugal projections in ferrets are very immature at birth (*2*); we reasoned that it might be possible to induce extensive plasticity in the retinothalamic pathway by surgery in neonatal ferrets.

Retinal targets were reduced in newborn ferret pups by ablating the superior colliculus and visual cortical areas 17 and 18 of one hemisphere (*3*) (Fig. 1). Ablating visual cortex causes the lateral geniculate nucleus (LGN) in the ipsilateral hemisphere to atrophy severely by retrograde degeneration. Concurrently, alternative target space for retinal afferents was created in the medial geniculate nucleus (MGN) by either ablating the inferior colliculus or sectioning fibers ascending to the MGN in the brachium of the inferior colliculus (*4, 5*).

Department of Brain and Cognitive Sciences, Massachusetts Institute of Technology, Cambridge, MA 02139.

*To whom correspondence should be addressed.

Experiments were done on 10 normal adult ferrets and 16 operated ferrets that were reared to adulthood. In five operated animals, intravitreal injections of anterograde tracers (*6*) revealed retinal projections to normal thalamic targets, including the surviving, shrunken LGN, as well as aberrant projections to auditory thalamic nuclei (Fig. 2). The new retinal projection zones included patches of the dorsal, medial, and ventral (or principal) divisions of the MGN, as well as parts of the lateral posterior nucleus and the posterior nuclear complex adjacent to the MGN. The retinal projections to the MGN complex occupied up to one-third of the volume of the MGN. We confirmed that the MGN in operated animals projected normally to auditory cortex (Fig. 1), both by the transneuronal label in auditory cortex after intraocular injections (*6*) and by the extensive retrograde labeling of cells in the MGN after restricted injections of horseradish peroxidase (HRP) or fluorescent retrograde tracers into primary auditory cortex (Fig. 2).

These experiments also indicated that the ipsilateral MGN is the major route for visual inputs to reach primary auditory cortex. Along with receiving major thalamic projections from the various divisions of the MGN (*7*), the primary auditory cortex in operated animals retained its connections with other auditory cortical areas. These included ipsilateral and contralateral connections with the second auditory area located lateral to primary auditory cortex and with areas on the ectosylvian gyrus located anterior, posterior, and ventral posterior to primary auditory cortex (*8*).

We next recorded responses of cells electrophysiologically from the MGN in operated animals (*9*) and compared visual responses there with responses from the surviving LGN in the same animals as well as from the LGN in normal animals. We studied the visual responses of single cells to various tests (*10*). We also tested the auditory responses of cells in the auditory thalamus with click or tone stimuli delivered through earphones.

In the LGN of normal animals, we recorded X, Y, and W cells (Fig. 3A); X and Y cells were found in the A laminae, and Y and

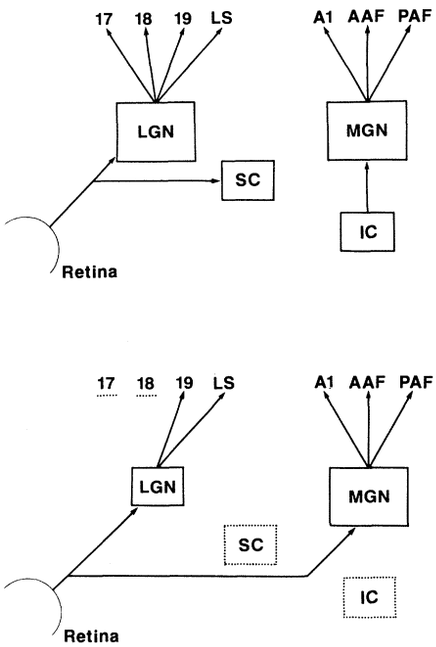

Fig. 1. The experimental design for induction of visual projections to the auditory system in ferrets. (**Top**) Projections in normal animals. The retina projects to LGN and superior colliculus (SC). The LGN projects to cortical areas 17 (primary visual cortex or striate cortex) and 18 as well as to other extrastriate areas including area 19 and the lateral suprasylvian (LS) cortex. In the auditory system, the inferior colliculus (IC) projects to the MGN. The ventral and the dorsal division of the MGN project heavily to primary auditory cortex (A1), as well as to other cortical areas including the anterior auditory field (AAF) and the posterior auditory field (PAF) in cortex (*29*). (**Bottom**) If cortical areas 17 and 18 are ablated in neonatal ferrets, the LGN atrophies severely by retrograde degeneration. Ablating the superior colliculus as well, and deafferenting the MGN by ablating the inferior colliculus or sectioning fibers ascending from it, causes the retina to project to the MGN and hence to auditory cortex.

Table 1. Visual cells recorded in primary auditory cortex of operated animals. Cells in primary auditory cortex were considered to receive retinal input if they were driven by electrical stimulation through electrodes implanted at the optic chiasm. They were then characterized by their responsiveness to visual stimuli.

Cell characteristic	Number of cells
Driven electrically from optic chiasm	57
Driven visually	38
Oriented receptive fields	6
Nonoriented receptive fields	23
Full-field flashes	9

W cells were found in the C laminae (*11*). In the LGN of operated animals, we recorded almost exclusively Y cells in the A laminae (Fig. 3B). We ascribe the loss of X cells in the LGN to the retrograde degeneration of geniculate X cells after ablation of visual cortex. A similar result has been shown in cats (*12*); in cats, neonatal visual cortical ablation also leads to transneuronal retrograde loss of X cells in the retina (*13*), and we have confirmed a reduction in medium-sized retinal ganglion cells in operated ferrets (*14*).

In the MGN of operated animals, we recorded cells with long latencies to optic chiasm stimulation (Fig. 3C). The conduction latencies of cells in the MGN of operated animals (range of latencies 2.8 to 11.0 ms, mean latency 4.8 ms, for 94 cells in five animals) were significantly longer than the latencies of X and Y cells in the LGN of normal animals (range of latencies 1.5 to 3.0 ms, mean latency 2.0 ms, for 101 cells in five animals; $P < 0.005$, Mann-Whitney U test, for a comparison of mean latencies in individual normal and operated animals). The visual responses of cells in the MGN were often variable or "sluggish" (*15*); cells responded best to large, flashing, or moving spots of light. Receptive fields were large, with diameters that were two to five times the diameters of normal LGN X cell receptive fields and up to twice the diameter of LGN Y cell receptive fields at similar eccentricities. Neurons dorsal in the MGN represented the upper visual field, neurons located ventrally represented lower visual field, neurons located medially represented central visual field, and those located laterally represented peripheral field. Receptive fields were on, off, or on-off center and circular. Visually driven cells were not orientation selective, although 2 of 32 visual units were direction selective (*16*). We used HRP to retrogradely fill retinal ganglion cells that projected to the LGN or superior colliculus in normal animals and to the LGN or MGN in operated animals (*17*). In normal adult ferrets, retinal ganglion cells include large-sized α (Y-like) cells that project to the LGN and superior colliculus, medium-sized β (X-like) cells that project mainly to the LGN, and a heterogeneous population of small and medium-sized (W-like) cells that project to the LGN and to the superior colliculus (*18*). In operated ferrets, the projection to the MGN arose mainly from the small retinal ganglion cells with heterogeneous morphologies (Fig. 3D). Our physiological and anatomical results thus suggest that the retinal ganglion cells that project to the MGN in operated animals belong to the W class. However, we cannot rule out the possibility that at least some cells that give rise to the aberrant projection are X or Y cells that fail to develop normally.

We also recorded from single units in primary auditory cortex of operated animals to determine their visual response features. Visual responses were strongest in the middle layers, at depths of 600 to 900 μm. In primary auditory cortex, as in the MGN, cells had long latencies to optic chiasm stimulation; the latencies ranged from 5.5 to 17.0 ms, with a mean latency of 9.0 ms (57 cells recorded in six operated animals). For comparison, latencies to optic chiasm stimulation in primary visual cortex of normal animals, which is dominated by the moderate- and fast-conducting X and Y pathways through the LGN (*1*), ranged from 2.0 to 6.5 ms, with a mean latency of 4.2 ms (63 cells recorded in four normal animals). The latencies in normal animals were significantly shorter than those in operated animals ($P < 0.005$, Mann-Whitney U test, for a comparison of mean latencies in individual animals). Cells in primary auditory cortex that were driven by visual stimulation formed a subset of the cells that were driven by electrical stimulation of the optic chiasm (Table 1). Visual cells in auditory cortex had large receptive fields and preferred slowly flashing or moving large spots or bars. As in the MGN, receptive fields were confined to the contralateral hemifield (*19*). About 25% of the cells that we could drive visually (10 of 38 units) showed direction selectivity. About 20% of cells showed orientation selectivity (Table 1) (Fig. 4) (*20*). All of the oriented cells had coextensive on and off

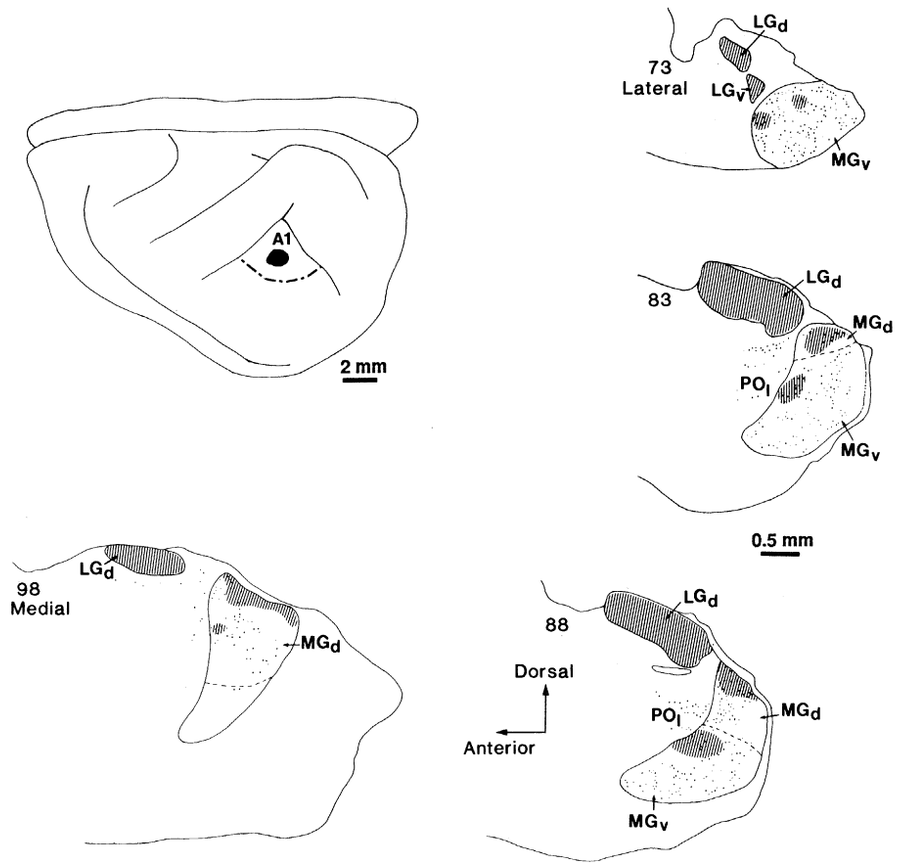

Fig. 2. Experimentally induced retinal projections (hatched areas) to the auditory thalamus and the connections of auditory thalamus with auditory cortex. The eye contralateral to the operated hemisphere projects to the surviving dorsal LGN (LG_d) and ventral LGN (LG_v) as well as to patches within the dorsal and ventral divisions of the MGN (MG_d and MG_v, respectively). Numbered parasagittal sections of the thalamus are shown. In the same animal, an injection of HRP in primary auditory cortex (A1) (the injection site is shown at top left) fills cells (indicated by dots) retrogradely in MG_v, MG_d, and the lateral division of the posterior complex (PO_l). Many cells in MG_d and MG_v overlie the retinal projection zone.

zones and responded to light onset and offset or to light and dark edges, and we classified them as complex (*21, 22*).

We could drive few neurons in the MGN or primary auditory cortex of the operated hemisphere with acoustic stimuli. This result was not unexpected because we had deafferented the MGN, but it confirmed that severed axons did not regenerate from the inferior colliculus to the MGN, at least not in large numbers. We could reliably elicit auditory responses from the MGN and primary auditory cortex in the unoperated hemisphere. We could not elicit responses to either electrical stimulation of the optic tract or visual field stimulation from cells in primary auditory cortex in normal animals (n = 48 single and multiple units) (*23*).

These results demonstrate that retinal projections can be induced to grow into nonvisual thalamus in ferrets and that these projections can impart visual function (that is, visual driving and discernible receptive field properties) to cells in nonvisual thala-

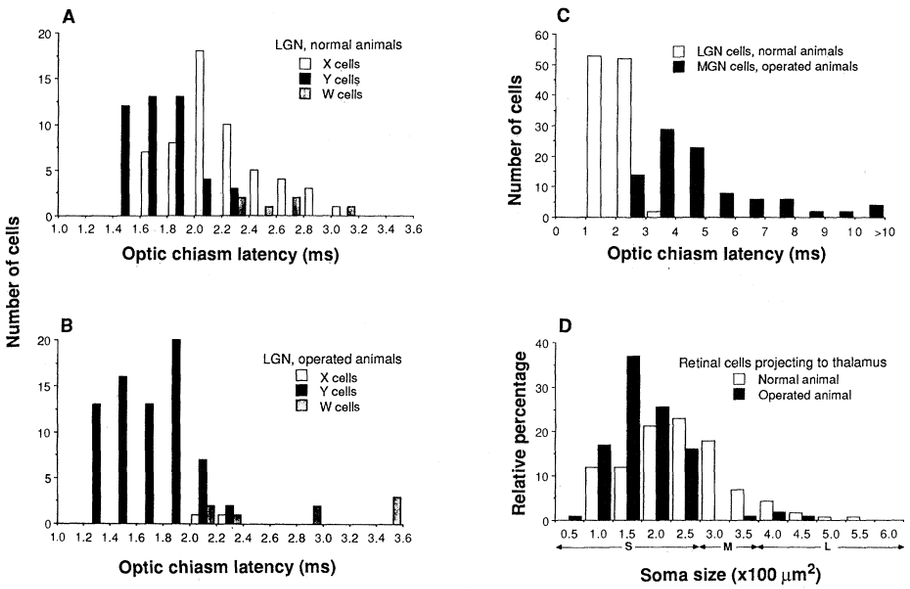

Fig. 3. Electrophysiological results from the thalamus of operated and normal animals and anatomical labeling of retinal ganglion cells that provide input to the thalamus in these animals. (**A**) The distribution of the latencies of firing, after electrical stimulation of the optic chiasm, of X, Y, and W cells in the LGN of normal animals. The histogram includes 107 cells pooled from five animals. X and Y cells are found in the A laminae, whereas the C laminae contain Y and W cells (*11*). (**B**) The LGN of operated animals contains Y cells (found in the A and C laminae), along with W cells (found in the C laminae), but very few X cells. Data are from 81 cells pooled from five animals. (**C**) Cells in the MGN of operated animals (94 cells in five animals) have long latencies to optic chiasm stimulation compared to cells in the LGN of normal animals [same data as in (A)]. (**D**) Histogram of soma sizes of retinal ganglion cells filled retrogradely from an HRP injection in the thalamus of a normal animal and an operated animal. The injection in the normal animal was centered on the LGN, and the injection in the operated animal was centered on the MGN. Each bar in the histogram represents the ganglion cells in a given size range as a percentage of the total population of backfilled cells. Retinal input to the thalamus in normal ferrets (*18*) arises from α or Y-like cells [these are, in general, large (L) cells with soma sizes of 400 μm² and larger), β or X-like cells [generally medium (M)-sized cells with soma sizes between 300 and 400 μm²), and a heterogeneous population of W-like cells [generally small (S) cells with soma sizes smaller than 300 μm², although this class can include medium-sized cells as well]. In operated ferrets, the cells that project to the MGN lie mainly in the small size range.

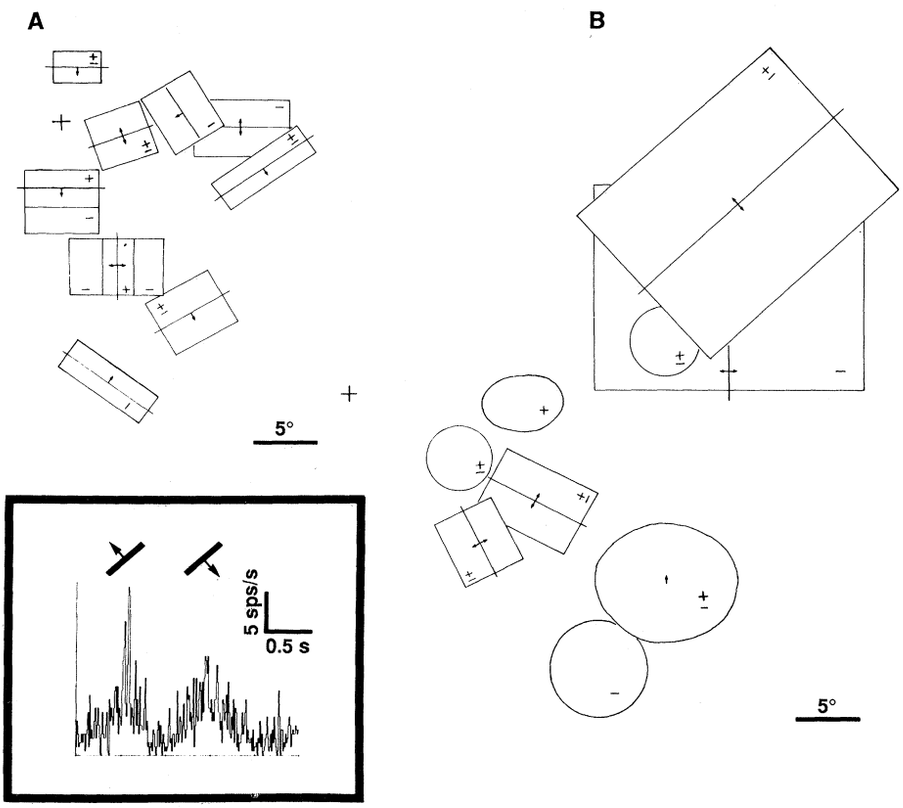

Fig. 4. Receptive fields of visual cells in primary auditory cortex of an operated animal with visual projections induced into the auditory system and comparison with receptive fields in primary visual cortex of a normal animal. Cells were classified as nonoriented or oriented simple or complex according to the criteria of Hubel and Wiesel (*21*). Simple cells have oriented fields with separate on (+) and off (−) zones, whereas complex cells have oriented fields usually with coextensive on and off zones. (**A**) Cells recorded in area 17 of a normal animal. Receptive field locations shifted progressively higher in the visual field as recording locations moved from dorsal to ventral in area 17, consistent with the map of visual space in area 17 in ferrets (*30*). The cross denotes the location of the area centralis. Small arrows within the receptive field denote the direction of stimulus movement yielding maximal response. Oriented line within each receptive field extending beyond receptive field edges denotes lack of end-stopping; lines that terminate at receptive field edges indicate end-stopped fields. (**B**) In primary auditory cortex of an operated ferret, visual cells had either nonoriented (circular) or oriented (rectangular) receptive fields. The oriented fields were complex-like. Receptive fields moved from dorsal to ventral in the visual field as recording locations moved from posteromedial to anterolateral in auditory cortex. (Inset) Peristimulus time histogram of a visual cell in primary auditory cortex responding to a bar sweeping across the receptive field at the orientation and directions indicated above the histogram. Bar width, 1°; bar length, 20°; velocity, 5°/s; 50 stimulus sweeps; sps/s, spikes per second.

mus and cortex. We suggest that, at least early in development, the modality of sensory thalamus or cortex can be specified by its inputs. Unlike rodents that have transient retinal projections to nonvisual thalamus that can be made permanent (*24*), in newborn ferrets the retina does not project to auditory thalamus (*25*). The novel retinal projections to the auditory thalamus thus represent sprouting from retinofugal fibers. If temporal factors play a role in the plasticity we describe, those retinal ganglion cells that have yet to establish stable thalamic or midbrain connections at the time of the lesions—including the smaller retinal ganglion cells that are generated last in the retina (*26*)—would be the most likely to innervate novel targets. Thus, surgery performed even earlier in development might induce more ganglion cells and perhaps other ganglion cell classes to reroute their axons as well. Alternatively, only certain retinal axons, intrinsically different from others, may be able to recognize cues in the denervated MGN and sprout into the nucleus.

Apart from the retinal cell classes that are involved in novel projections to the auditory system, our experiments provide a direct comparison of visual responses of neurons in the normal visual pathway with those induced into a pathway through nonvisual thalamus to cortex resembling those in primary visual cortex. Ideally, an evaluation of visual response features in primary auditory cortex and in normal striate cortex, for example, should involve cells that receive input from the same class of retinal ganglion cell in both structures (*27*). Still, our experiments suggest that some of the transformations on visual input performed in visual structures such as primary visual cortex in normal animals are possible as well in the primary auditory cortex in operated animals. One possibility consistent with our results is that visual inputs induce the development of specific intrinsic connections in primary auditory cortex resembling those in primary visual cortex. An alternative possibility is that intrinsic processing in primary auditory cortex may be similar in certain respects to that in primary visual cortex. This similarity might allow auditory cortex to process visual information; indeed, a parsimonious explanation of our results is that primary areas of sensory neocortex perform certain similar, stereotypical operations on input regardless of modality (*28*).

REFERENCES AND NOTES

1. Major features of organization of the retinogeniculate and geniculocortical pathways in mustelids (for example, ferrets and mink), which are carnivores like cats, have been described [R. W. Guillery and M. D. Oberdorfer, *J. Comp. Neurol.* **176**, 515 (1977); M. P. Stryker and K. R. Zahs, *J. Neurosci.* **3**, 1943 (1983); S. K. McConnell and S. LeVay, *J. Comp. Neurol.* **250**, 109 (1986); S. LeVay, S. K. McConnell, M. B. Luskin, *ibid.* **257**, 422 (1987)]. A review of the visual pathway in cats is given by S. M. Sherman and P. D. Spear [*Physiol. Rev.* **62**, 738 (1982)].
2. Ferrets are born after 41 days of gestation compared to 64 days for cats. At birth, the development of the retinogeniculate pathway in ferrets [D. C. Linden, R. W. Guillery, J. Cucchiaro, *J. Comp. Neurol.* **203**, 189 (1981)] resembles that in cats at about embryonic day 41 [C. J. Shatz, *J. Neurosci.* **3**, 482 (1983); D. W. Sretavan and C. J. Shatz, *ibid.* **6**, 234 (1986)], and subsequent retinofugal development in ferrets matches that in cats almost on a day-by-day basis.
3. Our basic surgical procedure is modified from that described for hamsters by G. E. Schneider [*Brain Behav. Evol.* **8**, 73 (1973)]; see also D. O. Frost [*J. Comp. Neurol.* **203**, 227 (1981)].
4. On the day of birth, ferret pups were anesthetized by hypothermia. An incision was made to expose the skull, and a flap of bone over visual cortex and superior colliculus of one hemisphere was removed. Visual cortex corresponding to areas 17 and 18 and the superior colliculus were then ablated unilaterally by cautery. In some animals, the inferior colliculus was ablated; in other animals, ascending auditory fibers in the brachium of the inferior colliculus were sectioned at the level of the midsuperior colliculus by inserting a blade coronally in the lateral portion of the midbrain. The scalp incision was sutured, and pups were revived and returned to the litter for rearing to adulthood.
5. In control experiments, we have examined the necessary and sufficient conditions for inducing retinal projections to auditory thalamus. Retinal fibers do not enter the MGN unless it is deafferented. Ablating the superior colliculus alone, along with deafferenting the MGN, causes a weak projection to the MGN. The projections are much heavier if visual cortex is ablated as well. We have been unable to induce retinal projections into nonvisual thalamic structures in cats by neonatal surgery, perhaps because by the time of birth, the retinal axons of cats have already grown into their target visual structures.
6. Adult ferrets were anesthetized with 2 to 3% halothane or with a mixture of ketamine (30 mg/kg) and xylazine (2 mg/kg). Intraocular injections were made with 15 to 25 μl of either wheat germ agglutinin conjugated to HRP (2%) or [^{35}S]methionine (500 μCi) dissolved in saline. Survival times ranged from one to several days. Animals were then deeply anesthetized and perfused intracardially with saline followed by a mixture of 1% paraformaldehyde and 2% glutaraldehyde. Frozen sections (50 μm) were cut in the parasagittal or coronal plane and processed for visualization of HRP [M.-M. Mesulam, *J. Histochem. Cytochem.* **26**, 106 (1978); J. C. Adams, *Neuroscience* **2**, 141 (1977)] or for autoradiography.
7. R. A. Andersen, P. L. Knight, M. M. Merzenich, *J. Comp. Neurol.* **194**, 663 (1980); J. C. Middlebrooks and J. M. Zook, *J. Neurosci.* **3**, 203 (1983).
8. S. L. Pallas *et al.*, *Neurosci. Abstr.* **14**, 460 (1988).
9. Physiological experiments were done on 12 operated ferrets and 8 normal ferrets. Animals were anesthetized, paralyzed, and artificially respired. The eyes were refracted and focused on a tangent screen 114 cm in front of the animal. Stimulating electrodes were placed across the optic chiasm. Cells in the LGN and MGN, or in visual and auditory cortex, of normal and operated animals were recorded with glass micropipettes or parylene-insulated tungsten microelectrodes. Electrolytic lesions were made during recording with metal electrodes, and these lesions as well as electrode tracks were reconstructed and compared with architectonic regions to locate recording sites within the LGN and MGN, or within primary visual and primary auditory cortex.
10. Parameters we studied included receptive field size, latency to optic chiasm stimulation, linearity of spatial summation within the receptive field, time course of response to a stationary stimulus, and response to a fast-moving disk of contrast appropriate for the surround. These tests have been used to classify W, X, and Y cells in the cat LGN [C. Enroth-Cugell and J. G. Robson, *J. Physiol. (London)* **187**, 516 (1966); S. Hochstein and R. M. Shapley, *ibid.* **262**, 237 (1976), and M. Sur and S. M. Sherman; *J. Neurophysiol.* **47**, 869 (1982)]. We also studied the responses of cells to stationary flashed bars at different orientations and to spots moving in different directions at different velocities. For 19 visually responsive MGN cells, peristimulus time histograms were generated in response to a drifting or counterphasing sine-wave grating or a bar moving at different orientations and velocities.
11. M. Esguerra, P. E. Garraghty, G. S. Russo, M. Sur, *Neurosci. Abstr.* **12**, 10 (1986).
12. M. A. McCall *et al.*, *ibid.*, p. 591.
13. L. Tong *et al.*, *Science* **217**, 72 (1982).
14. M. Sur, A. W. Roe, P. E. Garraghty, *Neurosci. Abstr.* **13**, 590 (1987).
15. B. G. Cleland and W. R. Levick, *J. Physiol. (London)* **240**, 421 (1974).
16. None of 12 X and 16 Y cells in the LGN of normal animals and 19 Y cells in the LGN of operated animals showed orientation or direction selectivity.
17. HRP (30% in saline) was iontophoresed into physiologically identified sites in the LGN, superior colliculus, or MGN. After 24 to 48 hours of survival, animals were perfused with 1% paraformaldehyde and 2% glutaraldehyde. The retinas were dissected, reacted with *O*-dianisidine [J. S. De Olmos, *Exp. Brain Res.* **29**, 541 (1977)], and flat-mounted on slides. Retrogradely filled retinal ganglion cells were examined under a ×50 objective, and their soma areas were measured.
18. D. J. Vitek, J. D. Schall, A. G. Leventhal, *J. Comp. Neurol.* **241**, 1 (1985); A. W. Roe, P. E. Garraghty, M. Sur, *Neurosci. Abstr.* **13**, 1023 (1987). Central projections of retinal ganglion cells in ferrets are similar to those in cats [A. G. Leventhal, R. W. Rodieck, B. Dreher, *J. Comp. Neurol.* **237**, 216 (1985); L. R. Stanford, *J. Neurophysiol.* **57**, 218 (1987)].
19. This finding is consistent with the fact that there are no visual inputs into primary auditory cortex through the corpus callosum from visual areas in the contralateral hemisphere.
20. For each neuron showing orientation or direction selectivity, we defined the width of orientation or direction tuning as the range of orientations or movement directions to which the cell responded. Six visual units in primary auditory cortex that were orientation selective (Table 1) had orientation tuning widths of 60° to 120° (mean, 94°), and ten units that were direction selective had direction tuning widths of 60° to 180° (mean, 125°). In comparison, cells in striate cortex of three normal animals had orientation tuning widths of 30° to 90° (mean, 59°; $n = 27$) and direction tuning widths of 30° to 120° (mean, 85°; $n = 19$). No orientation-selective neuron in primary auditory cortex showed end-inhibition, but 7 of 27 units in normal striate cortex were end-inhibited (see also Fig. 4).
21. D. H. Hubel and T. N. Wiesel, *J. Physiol. (London)* **160**, 106 (1962).
22. C. D. Gilbert, *ibid.* **268**, 391 (1977).
23. This finding confirms experiments on localization in the cat cortex, including early experiments in which visual- and auditory-evoked potentials were recorded from the cortical surface [W. H. Marshall, S. A. Talbot, H. W. Ades, *J. Neurophysiol.* **6**, 1 (1943); R. F. Thompson, R. H. Johnson, J. J. Hoopes, *ibid.* **26**, 343 (1963)], that have distinguished primary auditory cortex as a region where only auditory and no visual responses can be recorded.
24. D. O. Frost, *J. Comp. Neurol.* **252**, 95 (1986); ——— and C. Metin, *Nature* **317**, 162 (1985).
25. D. C. Linden, R. W. Guillery, J. Cucchiaro, in (*2*); J. Hahm and M. Sur, *Neurosci. Abstr.* **14**, 460 (1988).
26. C. Walsh, E. H. Polley, T. L. Hickey, R. W. Guillery, *Nature* **302**, 611 (1983); C. Walsh and R. W. Guillery, *J. Neurosci.* **5**, 3061 (1985).
27. Whereas the visual projections through the MGN to primary auditory cortex in operated animals appear to arise chiefly from retinal W cells, visual inputs to striate cortex in normal animals arise from retinal X and Y as well as W cells. Although the literature on response properties of cells in normal visual cortex is extensive, little of it derives from cells with pure W cell input; however, see B. Dreher, A. G. Leventhal, and P. T. Hale [*J. Neurophysiol.* **44**, 804 (1980)].
28. Several lines of evidence support such a conclusion.

(i) Intrinsic interlaminar connections described for cat striate cortex [C. D. Gilbert and T. N. Wiesel, *Nature* **280**, 120 (1979); D. Ferster and S. Lindstrom, *J. Physiol. (London)* **342**, 181 (1983)] share fundamental similarities with those described for cat primary auditory cortex [A. Mitani *et al.*, *J. Comp. Neurol.* **235**, 430 (1985)]. (ii) Direction-selective neurons (responding to the direction and rate of sound frequency modulation) have been noted in primary auditory cortex [I. C. Whitfield and E. F. Evans, *J. Neurophysiol.* **28**, 655 (1965); J. R. Mendelson and M. S. Cynader, *Brain Res.* **327**, 331 (1985)]. In the somatosensory cortex, direction- and orientation-selective neurons analogous to those in striate cortex have been described [J. Hyvarinen and A. Poranen, *J. Physiol. (London)* **283**, 523 (1978); S. Warren, A. Hamalainen, E. P. Gardner, *J. Neurophysiol.* **56**, 598 (1986)]. A more general discussion of common aspects of processing in sensory cortex is by V. B. Mountcastle [*The Mindful Brain*, G. M. Edelman and V. B. Mountcastle, Eds. (MIT Press, Cambridge, 1978), pp. 7–50]. (iii) In our experiments, lesions are used to route retinal projections into the auditory thalamus, and the extrinsic and intrinsic connections of auditory cortex are not altered, at least directly. Other experiments provide evidence for target-controlled differentiation of synaptic structure during development [G. Campbell and D. O. Frost, *Proc. Natl. Acad. Sci. U.S.A.* **84**, 6929 (1987); P. Rakic, *Science* **241**, 170 (1988)], suggesting that the neuropil of primary auditory cortex in operated animals would resemble that in normal animals. Thus the fact that auditory cortex in operated animals can process visual information in a manner similar to normal visual cortex implies that at least some aspects of intrinsic processing are similar in visual and auditory cortex.

29. L. M. Aitkin, D. R. F. Irvine, W. R. Webster, in *Handbook of Physiology: The Nervous System*, I. Darian-Smith, Ed. (American Physiological Society, Bethesda, MD, 1984), vol. 3, pp. 675–737.
30. M. I. Law and M. P. Stryker, *Invest. Ophthalmol. Visual Sci. Suppl.* **24**, 227 (1985).

31. We thank A. Graybiel, P. Schiller, and G. Schneider for comments on the manuscript, D. Frost and P. Rakic for help and advice, and M. MacAvoy and T. Sullivan for technical assistance. Supported by NIH grants EY07023 and EY07719, March of Dimes grant 1-1083, and the McKnight Foundation.

4 August 1988; accepted 27 September 1988

Reconstitution and Phosphorylation of Chloride Channels from Airway Epithelium Membranes

HECTOR H. VALDIVIA, WILLIAM P. DUBINSKY, ROBERTO CORONADO

Airway epithelial chloride secretion is controlled by the apical-membrane chloride permeability. Purified apical-membrane vesicles from bovine tracheal epithelium have now been shown to contain functional chloride channels by using the planar-bilayer technique. Three types of chloride channels were observed; a voltage-dependent, calcium-independent, 71-picoSiemen (in 150 m*M* NaCl) channel accounted for more than 80 percent of the vesicular chloride conductance and was under strict control of phosphorylation. The channel underwent a fast rundown in less than 2 to 3 minutes of recording, and reactivation required in situ exposure to a phosphorylating "cocktail" containing the catalytic subunit of the adenosine 3′,5′-monophosphate (cAMP)–dependent protein kinase. Mean open time and open probability were increased after phosporylation, whereas slope conductance remained unchanged. Thus, metabolic control of tracheal chloride single channels can now be studied in vitro.

CHLORIDE SECRETION THROUGH apical-membrane airway epithelium is a central process in respiratory tract fluid formation and mucociliary clearance. In cystic fibrosis (CF), a generalized exocrinopathy characterized by impaired Cl^- secretion (*1*), concentrated mucus collects in the respiratory tract and leads to recurrent infection, ultimately causing patient death. In normal cells, Cl^- accumulates against its electrochemical equilibrium via a co-transport mechanism (Cl^--Na^+ and possibly Cl^--K^+) located in the basolateral membrane. Chloride leaves the cell through apical membrane Cl^- channels, diffusing down its electrochemical gradient (*2*). A variety of hormones, neurotransmitters, and pharmacological agents with mechanisms of action that are mediated by elevation of Ca^{2+} (*3*) or cAMP (*4*) leads to an increase in Cl^- secretory activity. Electrophysiological studies in human tracheal epithelium have shown that cAMP promotes opening of Cl^- channels by a mechanism that involves phosphorylation of the channel protein or of a closely associated protein (*5*). Direct exposure of human tracheal cell patches to a phosphorylating "cocktail" containing the catalytic subunit of cAMP-dependent kinase results in opening of Cl^- channels in normal but not in CF tissue. Thus the phosphorylation target of protein kinase A is the most likely site of the defect in CF (*5*). As a first step to identify this phosphorylation site in Cl^--secreting epithelium, we developed an in vitro assay for Cl^- channels where purified components can be selectively added. We report the use of planar bilayers (*6*) to record phosphorylated and nonphosphorylated forms of the Cl^- channel of purified apical-membrane vesicles of bovine trachea (*7*). The method requires little material compared to isotopic flux measurements (*8*), and membrane vesicles can be stored frozen for weeks without loss of Cl^- channel activity.

We encountered five channel types in six different membrane preparations of bovine trachea (Table 1). In 15 of 56 recordings we observed two anion-selective types (52 and 140 pS) and two cation-selective types (83 and 201 pS). Anion and cation channels were identified as such on the basis of reversal potentials in asymmetric solutions. The anion-selective channels were sensitive to 4,4′-diisothiocyanostilbene-2,2′-disulfonate (DIDS) (*9*), and cation-selective channels were sensitive to amiloride at high concentration (>2 m*M*). The 52-pS anion channel showed strong rectification and an open probability that increased at positive potentials. The 140-pS anion channel remained open at all tested potentials. In 40 of 56 recordings we observed a 71-pS anion channel, which is the focus of this report. A large osmotic gradient across the planar bilayer was crucial in the detection of this

Table 1. Channel types in purified bovine airway epithelium membranes. *n*, total number of recordings of the channel type. Slope conductance was measured near the reversal potential (E_{rev}) for the indicated NaCl gradient. Permeability ratios (P_{Cl}/P_{Na}) were calculated from the Goldman equation without correction for ionic activities. Results from successful recordings (n = 56) from a total of 72 trials from six membrane preparations are shown.

Type	Conductance (pS ± SD)	E_{rev} (mV ± SD)	P_{Cl}/P_{Na} or P_{Na}/P_{Cl} (± SD)	[NaCl] (*M*) (cis/trans)	*n*
Anion	130 ± 12	+20 ± 2.5	15 ± 5	0.41/0.16	40
	71 ± 4	0	–	0.15/0.15	2
Anion	52 ± 5	+12 ± 1.2	4 ± 0.2	0.41/0.16	5
Anion	140 ± 6	+18 ± 0.8	7 ± 0.5	0.41/0.16	2
Cation	83 ± 2	−27 ± 0.4	50 ± 3	0.45/0.15	4
Cation	201 ± 10	−50 ± 2.4	>100	0.35/0.05	4

H. H. Valdivia and R. Coronado, Department of Physiology and Molecular Biophysics, Baylor College of Medicine, Houston, TX 77030.
W. P. Dubinsky, Department of Physiology and Cell Biology, University of Texas, Health Science Center at Houston, Houston, TX 77225.